

# Kinetics and Mechanism of Microtubule Length Changes by Dynamic Instability\*

(Received for publication, November 16, 1987)

Michael Caplow, John Shanks, Scott Breidenbach, and Richard L. Ruhlen

From the Department of Biochemistry, University of North Carolina, Chapel Hill, North Carolina 27599-7260

Microtubules at steady state were found to undergo dramatic changes in length, with only very little change in number concentration and mean length. This result is accounted for by a mechanism in which microtubules are capped at ends by tubulin-GTP subunits; loss of the tubulin-GTP cap at one end results in disassembly of all the tubulin-GDP subunits, so that the medial edge of the distal tubulin-GTP cap is exposed; the exposed tubulin-GTP cap is sufficiently stable, so that microtubule regrowth from the cap rather than loss of the cap occurs. This mechanism predicts that a bell-shaped length distribution of sheared microtubules will be transiently bimodal, with peaks of short and moderate length microtubules, in rearranging to an exponential length distribution. We have observed the predicted transient bimodal length distribution experimentally and in a Monte Carlo simulation.

Dynamic instability has recently been accounted for by assuming that microtubule ends are capped with only a single tubulin-GTP subunit at each end of the five helices that serve as elongation sites. Such a minimal tubulin-GTP cap is apparently ruled out by our observations, which require that the remnant tubulin-GTP cap generated from disassembly be able to serve as nucleating site; we do not expect that a stable nucleating site can be generated from five tubulin-GTP subunits, oriented as the five helices that serve as elongation sites.

Microtubule dynamic instability allows for dramatic shortening of a small subpopulation of microtubules, under conditions where the remaining microtubules progressively elongate (1). Because the dynamic instability model results in significant changes in microtubule lengths, it is an attractive one for accounting for the large changes in the microtubule cytoskeleton during the cell cycle. The magnitude of the length changes associated with dynamic instability behavior has, however, been open to question. The mean excursions in length seen in darkfield microscopy measurements of disassembling microtubules (2) was only 0.73  $\mu\text{m}$  at the minus end and 2.4  $\mu\text{m}$  at the plus end. Furthermore, it has been found (3) that sheared steady-state microtubules increase to a limiting length, equal to about 3.5 and 50  $\mu\text{m}$ , respectively, in the presence and absence of MAPs.<sup>1</sup> A limiting length is apparently reached because excursions in length are finite for

microtubules in the disassembly regimen; if very long microtubules were able to disassemble fully, then lengths would not be limited. Additional evidence concerning the magnitude of excursions of disassembling microtubules was obtained from studies of the rate of recovery of fluorescence when fluorescent microtubules in cells were photobleached (4). It was found that the rate was slower when the bleached spot was far from the microtubule end. This indicates that in cells not all disassembling microtubules disassemble to completion.

We have recently studied the relaxation rate for assembly and disassembly of steady-state microtubules when these are rapidly heated from 34 to 37 °C (5). From analysis of the lag for attainment of a maximal assembly rate after a temperature increase, it was calculated that the half-time for recapping of disassembling microtubules was at least 20 s. Since disassembling microtubules have been found to lose about 4500 tubulin subunits/s, it is expected that the excursion in length for an uncapped disassembling microtubule will go to completion, so that the microtubule will disappear. There is, however, a reaction path in addition to recapping that may prevent a disassembling microtubule from disappearing. It was pointed out (6) that when a microtubule loses a tubulin-GTP cap at one end and thereby enters the disassembly regimen, the disassembly may ultimately be reversed when the inside edge of the distal tubulin-GTP cap is exposed. The disassembly can then bounce off the distal cap, allowing the microtubule to be retained. We here describe results implicating this mechanism, with microtubules formed from pure tubulin dimer. Our evidence that the tubulin-GTP cap can act as a nucleating site indicates that it is composed of more than a single row of subunits, oriented as the five helices that serve as elongation sites.

## MATERIALS AND METHODS

Beef brain microtubular protein, purified as described previously (7), was made free of MAPs using phosphocellulose (8). The protein was stored in 50 mM Pipes, 2 mM EGTA, 1 mM  $\text{MgSO}_4$ , pH 6.9; for assembly, the magnesium and GTP concentrations were increased to 7.5 and 1.5 mM, respectively. Tubulin (40  $\mu\text{M}$ ) was assembled at 37 °C, seeding the reaction mixture with a 1% volume of microtubules that had been assembled in the presence of 4 M glycerol and then sheared by passage through a syringe needle.

Elongation of axonemes by subunits released from sheared steady-state microtubules was with microtubules that had been assembled to a steady state from 35  $\mu\text{M}$  tubulin subunits. These were sheared by three passes through a narrow gauge needle into a water-jacketed syringe at 36 °C. In the last passage out of the syringe, 200  $\mu\text{l}$  were squirted into 15  $\mu\text{l}$  of a dilute solution of axonemes (from *Stronglyocentrotus purpuratus*, kindly provided by Dr. Mary Porter, University of Colorado).

Lengths of microtubules were determined by transmission electron microscopy of samples that were negatively stained with uranyl acetate. Aliquots of the reaction mixture were diluted into the buffer used for assembly (supplemented with 40% glycerol and 10% dimethyl sulfoxide) and then centrifuged on to an electron microscope grid, using an Airfuge and the Beckman EM90 rotor. Approximately 500

\* This work was supported by Grant DE03246 from the National Institutes of Health. The costs of publication of this article were defrayed in part by the payment of page charges. This article must therefore be hereby marked "advertisement" in accordance with 18 U.S.C. Section 1734 solely to indicate this fact.

<sup>1</sup> The abbreviations used are: MAPS, microtubule-associated proteins; EGTA, [ethylenedis(oxyethylenenitrilo)]tetraacetic acid; Pipes, piperazine-*N,N'*-bis(2-ethanesulfonic acid).

microtubules were measured, using a Zeiss digitizer for constructing a histogram of lengths. Spectrophotometric measurements of microtubule assembly and disassembly were measured as described elsewhere (5).

## RESULTS

*Contribution of Dynamic Instability to Microtubule Dynamics*—We have previously observed (5) that approximately 2% of a steady-state, MAP-free microtubule population is uncapped and disassembling and that disassembling microtubules are only very slowly recapped by reaction with tubulin-GTP subunits. It was, therefore, expected that, as observed previously (1), dynamic instability would rapidly decrease the microtubule number concentration in reactions that are at a steady state. In the studies described here, we looked for the change in microtubule length distribution resulting from dynamic instability in samples taken from a reaction shortly before and after it had attained a steady state. This was done because it has been reported that, apparently because disassembling microtubules can undergo a facile recapping reaction, the rates of increase in microtubule length and of decrease in microtubule number become very slow when microtubules are only moderately long (3). Thus, to be assured that we may observe length changes produced by dynamic instability, measurements were started as soon as possible after most of the assembly reaction was complete.

When tubulin polymerization was induced by seeding a preparation of pure dimer with sheared fragments of microtubules, the initial and steady-state product consisted of microtubules (Fig. 1). Nonmicrotubule polymers constituted 0.6–1.75% of the total mass of tubulin polymer (Fig. 1). That microtubules constituted the principal polymerization product in both samples was important, because we studied the kinetic properties of the initially formed and steady-state polymers (see below).

To determine the impact of dynamic instability on this microtubule population, lengths of microtubules were measured by electron microscopy at a point when the assembly reaction was approximately 80% complete (200 s) and later, about 500 s after attainment of a steady state. We were surprised to find that the mean microtubule length only

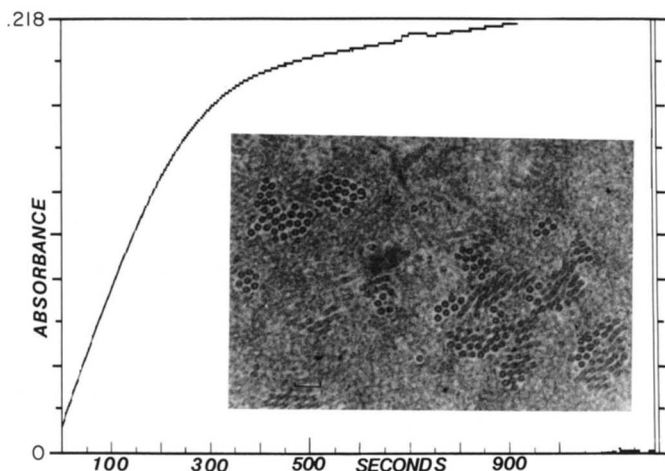


FIG. 1. Kinetics and products formed by polymerization of pure tubulin dimer. The inset shows a cross-section of the pellet obtained by centrifuging the reaction mixture in an Airfuge (30 s, 37 °C, 30 p.s.i.) 1000 s after inducing assembly; only 2 of 352 cross-sections had a nontubular shape. When the sample was incubated for for 100 s before centrifuging, 7 of 200 cross-sections were not tubular. The length of the bar in the inset figure is 0.1  $\mu\text{m}$ .

increased from 33.7  $\mu\text{m}$  at 200 s to 35.7  $\mu\text{m}$  at 925 s (Fig. 2).<sup>2</sup> There was, however, a difference in the length distribution of the microtubule populations 200 and 925 s after induction of assembly. The sample that had been incubated for a longer time appeared to have more very long and relatively short microtubules. The approximate constancy of the mean length indicated that dynamic instability had not significantly altered the microtubule number concentration. To confirm this we determined the initial rate of disassembly, following a rapid temperature shift to 1 °C. Since the disassembly rate is proportional to the number concentration of microtubule ends (9, 10), the initial rate was expected to be the same for the two reactions described in Fig. 2. In three experiments (Table I) the initial rate of disassembly (corrected for variations in the microtubule number concentration in different reactions; see right-most column in Table I) was actually slightly faster for the steady-state reaction, as compared to the pre-steady-state reaction. We believe that the slightly faster initial disassembly rate of the longer incubated samples resulted from experimental error. The fact that the initial rate was not reduced during the approximately 200–1000-s interval might be taken to indicate that dynamic instability is not important under the reaction conditions used here. However, it was noted that the shape of the plot describing the thermal-induced disassembly was dramatically different in reactions incubated for approximately 200 or 1000 s (Fig. 3): disassembly of the reaction that had incubated for approximately 1000 s continued for a much longer time. The longer reaction time required for disassembly indicated that at approximately 1000 s the reaction mixture contained a larger population of very long microtubules. A similar conclusion was derived from comparison of the length distributions determined by electron microscopy (Fig. 2).

*Kinetic Assay of the Microtubule Length Distribution*—It was noted by Johnson and Borisy (12) that, when microtubules are induced to disassemble, the derivative of the disassembly rate gives a profile of the lengths of the reacting microtubules. This concept is graphically described in Fig. 4. In a subsequent study, in which disassembly was induced by dilution and by chilling (9), it was demonstrated that microtubule disassembly is from ends only and that it is possible to determine the length distribution of microtubules from the disassembly kinetics.

We modified the spectrophotometric assay for measuring thermal-induced disassembly (9, 12) by using a heat exchanger that very rapidly cooled the microtubule reaction mixture, by using a highly sensitive spectrophotometer and by converting the output from the spectrophotometer to a digital form, so that the disassembly rate could be measured accurately. Since the absorbance was measured at 0.25-s intervals, a considerable quantity of data was available to estimate statistically both the temperature-induced disassembly rate and the derivative of this rate. The microtubule length distribution is determined from this derivative.

Microtubules disassembled rapidly when the temperature

<sup>2</sup> The increase in microtubule mass when the reaction is incubated for about 700 additional s requires an increase in microtubule lengths, that is at least as large as the increase in mass; a larger increase in length will occur if dynamic instability works to decrease the number concentration. We suggest that our failure to observe comparable increases in mean microtubule length and mass results from experimental error. It is extremely difficult to measure the length of very long microtubules, because these are likely to be tangled with other microtubules. As a result, long microtubules are ignored more frequently than short microtubules in measuring lengths. Thus, the mean length of the longer incubated sample, which has a larger fraction of very long microtubules, is likely to be underestimated.

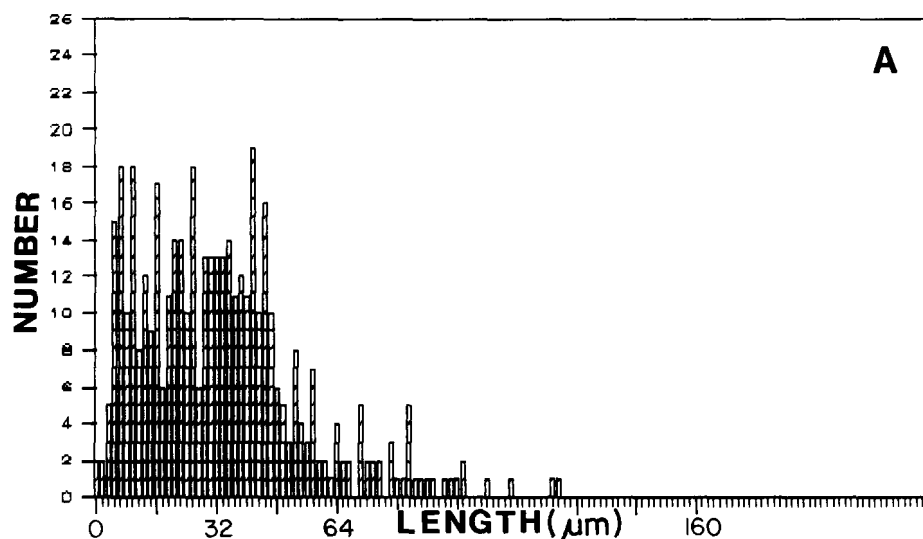
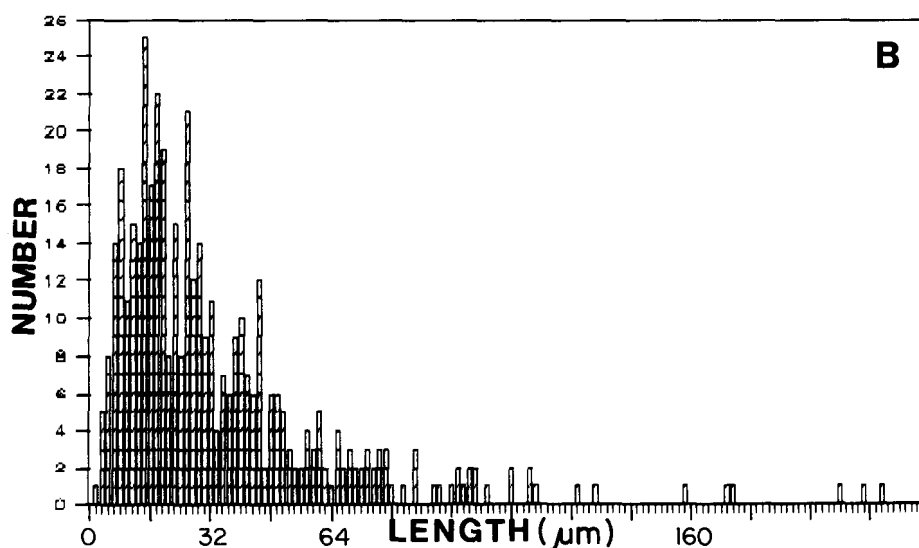


FIG. 2. Length distribution of microtubules 200 s (A) and 900 s (B) after inducing microtubule assembly.



was changed from 37 to 1 °C (Fig. 3). The disassembly reaction did not, however, reach a maximum rate until 15–20 s after the temperature shift was initiated. Although a part of the lag for attainment of a maximum rate resulted because the temperature change was not instantaneous, we have demonstrated that a 30-s lag for reaching a maximum disassembly rate following a temperature shift from 36 to 34 °C results because microtubules are apparently capped with stable tubulin-GTP subunits at their ends (5). A lag for attaining a maximum disassembly rate following a shift to 1 °C is, therefore, expected. The exact duration of the lag cannot, however, be predicted from the results at 36 and 34 °C, since the disassembly rate (and magnitude) is influenced by a difference in the effect of temperature on the assembly, disassembly, and GTPase rate constants (at each microtubule end). With appropriate effects of temperature on the various rate constants it is possible for the lag to be either longer or shorter at 1 °C, as compared to 34 °C.

Because the disassembly rate was not at a maximum for

15–20 s after the temperature shift, values of the second derivative were negative until this time. The kinetic method for determining lengths assumes that the disassembly rate will be at a maximum at the start of the reaction, since at this point all of the microtubules are still present. As a result, only positive second derivatives are expected. In our kinetic assay of lengths we discarded results from the period before the disassembly rate reaches a maximum; this corresponded to a point where 13–25% of the total microtubule mass had been lost. If it is assumed that the phenomenon that results in a lag in disassembly equally influences the disassembly of microtubule of all lengths, discarding the initial portion of the disassembly curve will result in underestimations of the fraction of short microtubules and the length of microtubules. The former results because the short microtubules that start to disassemble during the lag are especially likely to have disappeared before the disassembly rate reaches a maximum. The mean length of the microtubules is underestimated because the microtubules that are disassembling when the lag

TABLE I

Rate of thermal-induced disassembly of pre-steady-state and steady-state microtubules

Microtubule assembly was initiated in duplicate reaction by adding a 1% volume of sheared steady-state microtubules, formed in a glycerol-promoted reaction, to 35–40  $\mu\text{M}$  tubulin. It requires about 400 s for attainment of a steady state (see Fig. 1). At the indicated times the temperature was reduced from 37 to 1  $^{\circ}\text{C}$ , and the disassembly rate was measured.

Reaction no. <sup>a</sup>	Time initiated s	Absorbance change <sup>b</sup>	Disassembly rate <sup>c</sup>		
			Disassembly rate <sup>c</sup>	Assembly rate <sup>d</sup>	Disassembly rate/assembly rate <sup>e</sup>
			$A \times 10^4/\text{s}$		
1	200	0.127	35.7	6.26	5.7
	925	0.218	53.0	7.54	7.0
2	175	0.228	82.2	13.3	6.2
	1000	0.256	70.1	10.1	6.9
3	220	0.268	67.1	11.9	5.6
	1020	0.324	77.5	10.5	7.4

<sup>a</sup> Results from three separate reactions are given. In each, assembly was induced in two reaction mixtures, and disassembly was initiated at the indicated time.

<sup>b</sup> Total absorbance change induced by cooling to 1  $^{\circ}\text{C}$ .

<sup>c</sup> Maximum slope from a least squares analysis of the disassembly rate.

<sup>d</sup> The maximum assembly rate was determined from a least squares analysis of the slope of the pre-steady-state assembly reaction. The rate in individual reactions varied, because the number of seeds used to induce assembly apparently varied. The seeds were made in glycerol buffer, where end-to-end annealing rapidly reduced the seed concentration (11), making it difficult to construct identical reaction mixtures.

<sup>e</sup> The maximum disassembly rate is corrected for variations in the microtubule number concentration by dividing by the maximum initial pre-steady-state assembly rate.

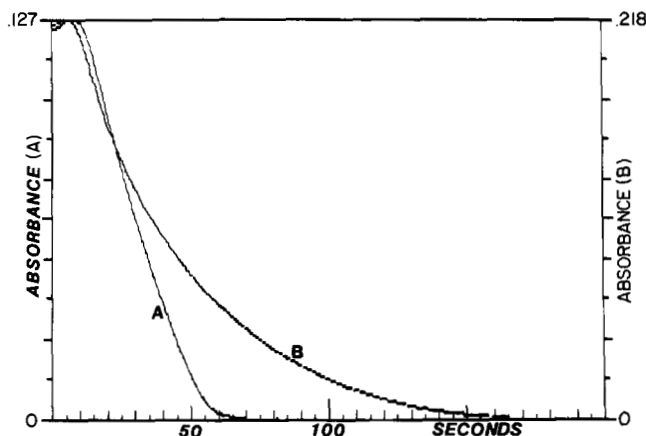


FIG. 3. Disassembly of microtubules at 1  $^{\circ}\text{C}$ . The microtubules formed in the reaction described in Fig. 1 were rapidly chilled at 200 s (A) or 925 s (B) after initiating assembly. This experiment is Reaction 1 in Table I.

is complete will have lost a fraction of their length by the time that the second derivative is zero; the just-described loss of very short microtubules serves to reduce further the measured mean from the true value. These errors in the kinetic assay of lengths are not expected to influence the conclusions from our studies, because the principal results involve relatively large changes in the size of a subpopulation of the longer microtubules. This population is not expected to be changed significantly by the factors described above. Finally, we believe that the kinetic assay of lengths is preferable to microscopy, since it is not necessary to correct for extensive shearing of longer microtubules during the sampling procedure (13).

Using the just-described kinetic assay to study the length

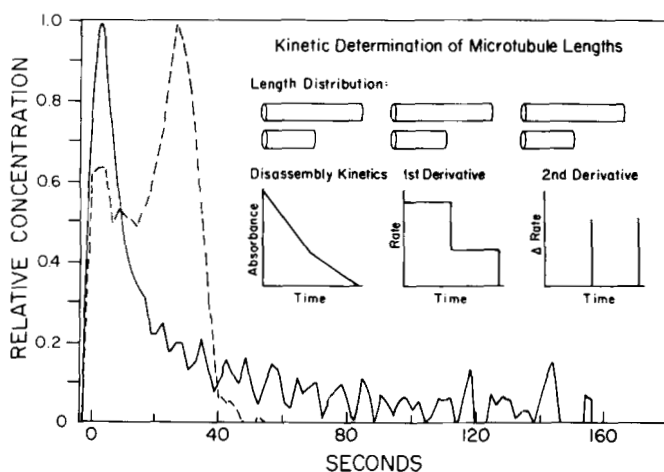


FIG. 4. Length distribution of microtubules before and after attainment of a steady state, and model (inset) for determining the microtubule length distribution from the kinetics for thermal-induced disassembly. In the model shown here we consider the rate of thermal-induced disassembly of a population of six microtubules, three long ones and three that are half as long. The rate of disassembly is twice as fast until the shorter microtubules have disappeared; at this point, two-thirds of the microtubule mass will have disassembled. The first derivative of the absorbance (i.e. the rate) is constant until the short microtubules disappear and until the long microtubules disappear. The second derivative of the absorbance shows a spike at the times when the short and long microtubules disappear. The abscissa for the second derivative plot can be converted to microtubule length, from knowledge of the disassembly rate in units of  $\mu\text{m}/\text{s}$ . Kinetic analysis of lengths for the reactions shown in Fig. 3 are shown here. Zero time on the abscissa corresponds to 20 s after the time when the cooling was initiated; the second derivative of the rate was negative for the first 16 s. The dotted line describes the 200-s reaction, and the solid line is for the 925-s reaction. Lengths are given in units of time, because we have not yet determined the rate of subunit dissociation at 1  $^{\circ}\text{C}$ ; preliminary results (unpublished) give a rate of about 1  $\mu\text{m}/\text{s}$ . Using time rather than length for describing the microtubule population is suitable for comparing microtubule populations under identical reaction conditions.

distribution of microtubules present 200 and 925 s after initiating assembly, it was found that there was a dramatic change during the 200–925-s interval (Fig. 4). The length distribution of the longer incubated sample was exponentially shaped, while the sample from the pre-steady-state reaction was bimodal, with an absence of very long microtubules. As noted above, the change in the distribution of microtubule lengths with time was not accompanied by a significant change in the microtubule number concentration.

**Disassembly of Sheared Microtubules**—Microtubules that were assembled to a steady state at 36  $^{\circ}\text{C}$  were rapidly cooled at 34  $^{\circ}\text{C}$ , and the relaxation rate for disassembly was measured (Table II and Fig. 5). After a new steady state was attained the temperature was rapidly increased to 36  $^{\circ}\text{C}$  and the relaxation associated with the assembly to the steady state at the higher temperature was recorded. This sequence was repeated. The relaxation rates for assembly and disassembly are expected to depend on the microtubule number concentration, so that an increase in the number concentration produced by shearing can be estimated by comparison of the relaxation rate for temperature-induced assembly or disassembly before and after shearing. Shearing was by rapid passage of the reaction mixture through a narrow gauge needle into a temperature-thermostatted syringe. Rigorous temperature control during this treatment was required, because assembly of MAP-free microtubules was exceedingly sensitive to temperature. As described previously (1), shearing resulted in massive disassembly of microtubules (Fig. 5), presumably because

TABLE II

Effect of shearing on the temperature-induced assembly and disassembly relaxation rate

Microtubules were assembled to a steady state at 36 °C (30 min), and the reaction was then rapidly cooled or heated, as described elsewhere (5). At the time indicated, microtubules were sheared by four rapid passes through a 26-gauge syringe needle in and out of a water-jacketed syringe at 36 °C. Rates were determined from an expanded plot of the slope of the absorbance trace shown in Fig. 7.

Time initiated	Temperature shift	Time rate maximal <sup>b</sup>	Maximum rate
s		s	$A \times 10^4/s$
30	36 → 34	68	4.52
300	34 → 36	338	3.77
550	36 → 34	588	3.92
820	34 → 36	860	3.63
Shear at 1055 s			
1275	36 → 34	1316	5.63
1470	34 → 36	1514	4.64

<sup>a</sup> Zero time corresponds to 30 min after assembly was initiated.

<sup>b</sup> We have previously found (5) that following a temperature jump approximately 30 s are required before the assembly or disassembly rate is maximal.

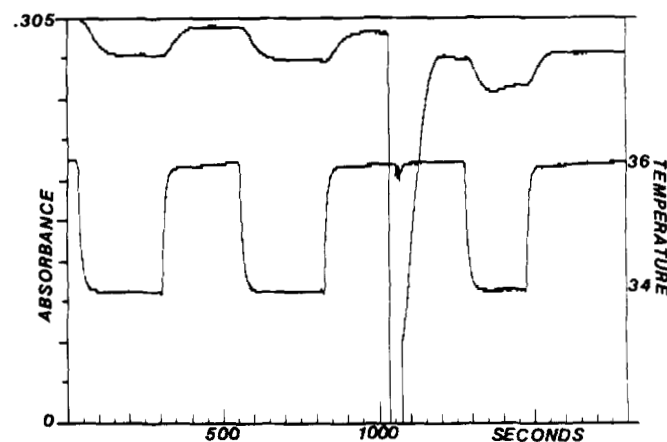


FIG. 5. Temperature-induced assembly and disassembly of microtubules before and after shearing. The upper trace describes the absorbance, and the lower trace describes the temperature, measured with a thermistor. Relaxation rates for assembly and disassembly are summarized in Table II. Shearing was done at 1055 s; note the very small temperature changes during the shearing.

exposure of tubulin-GDP subunits in the microtubule's interior allows disassembly that is ordinarily blocked by the presence of tubulin-GTP caps at the microtubule ends. Small bubbles in the reaction mixture made us uncertain about evaluating the kinetics of the assembly reaction that followed shearing; however, it was apparent that microtubule elongation occurred very rapidly. After about 150 s the bubbles had disappeared so that the sequence of temperature jumps that preceded shearing could be repeated. Surprisingly, 220 s after shearing, the relaxation rate for thermal-induced disassembly was only about 33% faster than before the microtubules were sheared (see right-most column in Table II). That the microtubules had been sheared by the flow through the syringe needle was indicated by the massive microtubule disassembly that accompanied the shearing. Also, the sheared microtubules were sampled directly from the flow from the syringe needle and these were found, by electron microscopy, to have a mean length of only 4.1  $\mu\text{m}$ ; before shearing, the mean length was 21  $\mu\text{m}$ . The minimal influence of shearing on the relaxation rate can be accounted for if it is assumed that the majority of microtubule fragments formed by shearing disassemble to completion. Loss of these potential seeds for micro-

tubule growth is likely, since we have found that tubulin-GDP subunits are lost from the microtubule ends at a rate of about 4500 subunits  $\text{s}^{-1}$ , and uncapped microtubules are only very slowly recapped by reaction with tubulin-GTP subunits (the half-time for recapping is at least 20 s (5)). Further evidence that the majority of microtubule seeds quantitatively disassembled was obtained by squirting the sheared microtubule mixture into a dilute solution of axonemes. When this reaction was sampled for electron microscopy after a 60-s incubation, the axonemes were found to be dramatically elongated. Assuming that elongation of an axonemal microtubule occurs to an extent identical to a microtubule fragment formed by shearing, it is necessary that the majority of the microtubule fragments disappear, so as to support the dramatic elongation that is observed. That is, if a significant fraction of the fragments formed by shearing did not disassemble to completion, then on average, these would be little elongated by the subunits released from uncapped microtubules. In summary, shearing generates fragments, the majority of which fully disassembled. Because the majority of fragments disappeared, the microtubule number concentration was not increased significantly by shearing.<sup>3</sup>

**Changes in the Length Distribution of Sheared Microtubules**—When microtubule lengths were measured 200 s after steady-state microtubules were sheared, the lengths appeared to be bimodally distributed (Fig. 6). Following an additional 700-s incubation, the medium length microtubules seemed to disappear, as longer microtubules were formed. This change in length distribution was accompanied by an only 48% change in mean length and microtubule number concentration (Fig. 6). Using the kinetic assay of microtubule lengths to confirm this observation, we found that 150 s after shearing, microtubule lengths had a unimodal distribution (Fig. 7), although a shoulder on the trailing edge of the peak hinted of a second peak of very short microtubules. At 225 s the distribution was bimodal, with peaks of short and moderate length microtubules. The latter peak became progressively smaller as it spread to longer lengths. At 900 s the length distribution had a peak of very short microtubules and an exponentially shaped population of longer polymers. Thus, the length distributions determined from electron microscopy and the kinetic assay agree. We also noted that the maximum disassembly rate, which is proportional to the microtubule number concentration, decreased by about 66%, during the 155–900-s period (see right-most column in Table III). This decrease is in good agreement with that determined from electron microscopy, which indicated a 48% decrease in the number concentration during the 200–900-s interval.

## DISCUSSION

We have previously found (5) that uncapped microtubules lose more than 4,500 subunits/s and that the half-time for recapping of uncapped microtubules is at least 20 s. Since the mean excursion for disassembly of an uncapped microtubule is equal to  $(t_{1/2} \text{ for recapping}) \times (\text{rate constant for subunit}$

<sup>3</sup> Because microtubules have only two tubulin-GTP caps, it might be expected that shearing will only double the microtubule number concentration, if fragments other than caps fully disassemble. However, the microtubule number concentration may increase significantly after shearing, if there is a pause between passes of the reaction mixture through the syringe needle. During the pause new nuclei may form from tubulin-GTP subunits, and the tubulin-GTP caps that form at each new microtubule end may elongate sufficiently, so that it is likely to be stable when liberated by subsequent shearing. Such caps will serve as nucleating sites for microtubule assembly, using the subunits released by shearing. This sequence will allow for a more than doubling in microtubule number concentration.

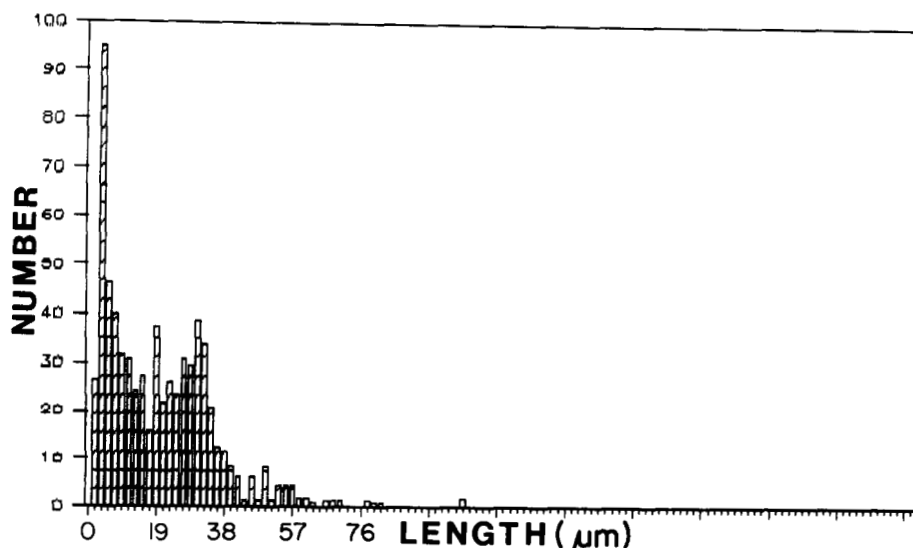
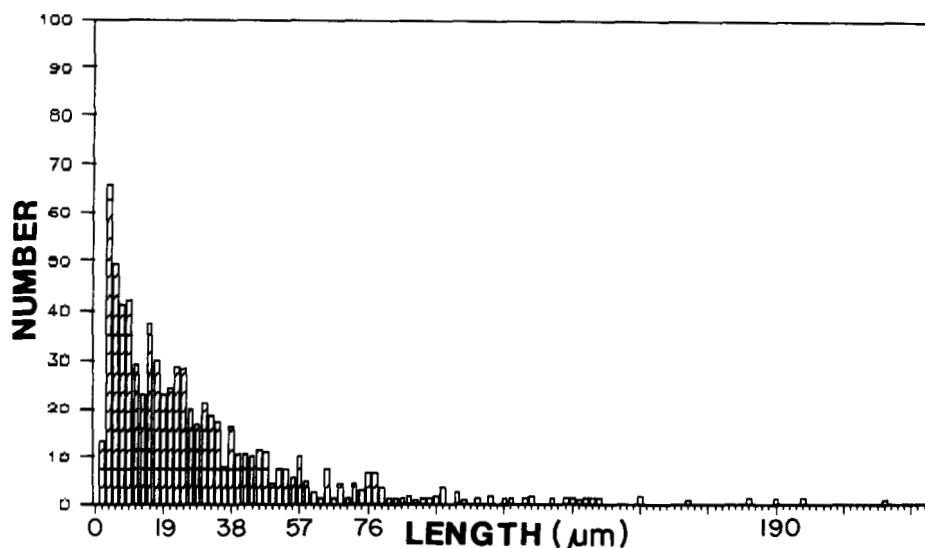


FIG. 6. Changes in the length distribution of microtubules after shearing. *A* and *B* are for the reaction 200 and 900 s after shearing. The mean length of the microtubules was  $16.7 \mu\text{m}$  in *A* (747 microtubules measured) and the mean length was  $24.7 \mu\text{m}$  in *B* (789 microtubules measured).



dissociation)/ $\ln 2$ ), it is calculated that a disassembling microtubule will lose 130,000 subunits ( $79 \mu\text{m}$ ), on average, before it is recapped. It would, therefore, be expected that uncapped microtubules would disassemble to completion.

Our observation that at steady state the microtubule number concentration and mean microtubule length remained relatively constant (Fig. 2, Table I, right-most column) indicates that either the population of uncapped microtubules is extremely small, or that some reaction other than recapping serves to modulate dynamic instability. The former possibility is apparently not correct, since we find that at steady state approximately 2% of the microtubule population is uncapped and disassembling (5). Also, if the population of uncapped microtubules is extremely small, then we would not observe a rapid change in length distribution (Figs. 2, 4, 6, and 7). We suggest that a reaction other than recapping serves to modulate dynamic instability.

A low recapping rate constant and relatively high population of uncapped microtubules (5) can be reconciled with the

observed rapid changes in length distribution (Figs. 2, 4, 6, and 7) by a mechanism (Fig. 8) in which uncapped disassembling microtubules are not recapped before they lose all tubulin-GDP subunits. This subunit loss exposes the inside edge of the tubulin-GTP cap at the opposite microtubule end; the tubulin-GTP subunits at the exposed edge are presumably able to support microtubule assembly. The effect of this reflection from the exposed cap is to prevent disappearance of the disassembling microtubule. Subunits released from disassembly of uncapped microtubules elongate the population of capped microtubules and these become progressively longer. According to this mechanism the length distribution will eventually be composed of microtubules that are either very long, because they have not recently undergone catastrophic disassembly, or relatively short, because they have recently disassembled to the point where the residual tubulin-GTP cap has acted as a nucleation center. A slow decrease in the microtubule number concentration results from disassembly of the tubulin-GTP caps that are released from disassem-

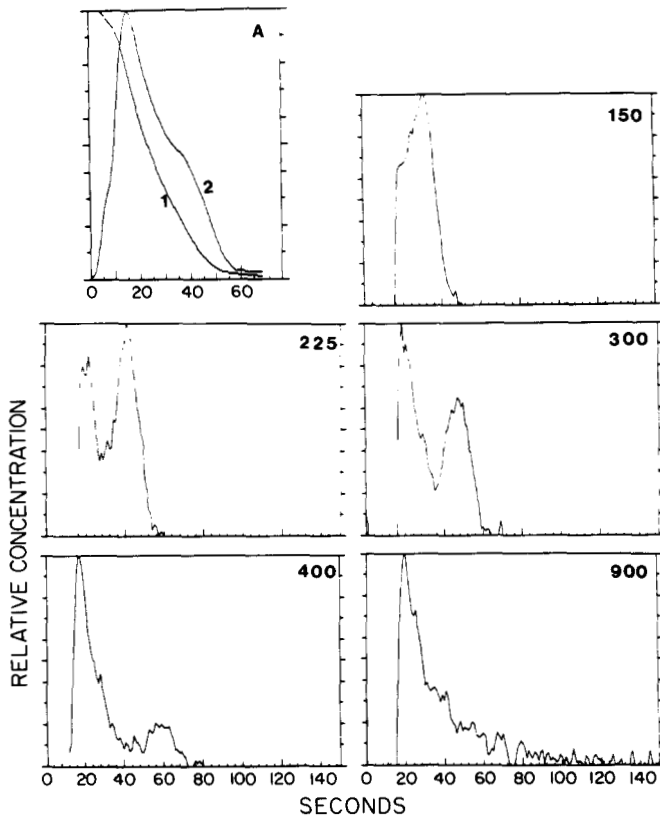


FIG. 7. Changes in the length distribution of microtubules after shearing. Curve 1 in A describes the absorbance as a function of time, when microtubules were chilled 225 s after shearing. Zero time on the *abscissa* corresponds to the time when the temperature change was initiated. Curve 2 in A describes the time dependence of the rate; the maximum rate (at about 16 s) was 0.0087 A/s. The shoulder on the curve generates the valley between the peak of short and moderate length microtubules (see 225 s results immediately below). Curves describing the derivative of the rate at the indicated times after shearing are also given; only positive values are shown. Zero time for the *abscissa* corresponds to the time when the temperature shift was started. Four of the five reactions shown here are further described in Table III. The absorbance change for the reaction at 400 s was 1.44 times that in the other four reactions, apparently because an error was made in making the microtubule reaction mixture; this would not be expected to influence the change in length distributions significantly. Comparable results were obtained in four additional experiments in which lengths were measured 150, 225, 300, and 900 s after shearing.

TABLE III

Thermal-induced disassembly rate of sheared steady-state microtubules

Microtubules at 36 °C were sheared and then incubated for varying times before being rapidly chilled to 1 °C. The disassembly rate was measured spectrophotometrically. The total absorbance change from the disassembly was 0.252.

Time after shearing	Mean length <sup>a</sup>	Median length <sup>a</sup>	Maximum rate
s	s	s	A × 10 <sup>2</sup> /s
150	30.7	29	1.28
225	35.8	36	0.87
300	36.6	33	0.90
900	40.5	30	0.77

<sup>a</sup> Lengths are expressed in units of seconds; this could be converted to microns by multiplying by the disassembly rate (μm/microtubule/s), which has not been determined. Lengths expressed in time units are valid for comparison purposes.

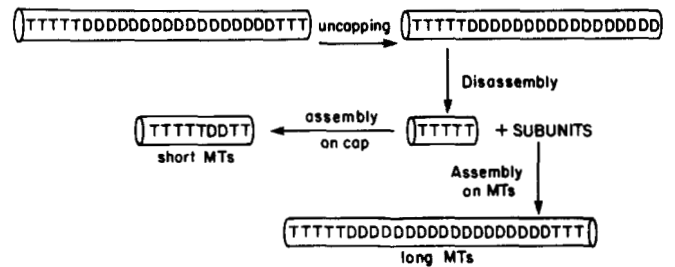


FIG. 8. Mechanism for changes in the length distribution of steady-state microtubules (MTs), under conditions where there is little change in microtubule number concentration. It is expected that steady-state microtubules will lose a cap at only one end, so that the tubulin-GTP cap at the opposite end will be available for reaction with tubulin-GTP subunits. In a previously proposed reaction scheme (Fig. 2 in Ref. 6) the tubulin-GTP cap that is exposed by disassembly is involved in a competition between a reaction in which tubulin-GTP subunits elongate the exposed cap (the  $J_{11}$  path) and disappearance of the exposed tubulin-GTP cap (the  $\gamma$ -path). Since under the conditions used here exposed tubulin-GTP caps only rarely undergo disassembly, we have simplified this scheme by omission of the  $\gamma$ -path.

bling microtubules and from the small population of microtubules that become uncapped at both ends. A reaction of a remnant tubulin-GTP cap with tubulin-GTP subunits was previously recognized as of potential significance for influencing microtubule dynamics (6). There was, however, no previous evidence implicating this reaction path with steady-state microtubules.

*Monte Carlo Simulation of Length Changes*—Chen and Hill (14) have used a Monte Carlo simulation to analyze the change in length and number of steady-state microtubules. The rate constants used for this simulation were derived from the slope and intercept of a plot of rate of axoneme elongation, as a function of tubulin subunit concentration (1), and from an empirical fit of the dependence of the flux rate on the tubulin subunit concentration, in a Monte Carlo simulation of assembly and disassembly from a five-start helix (15). To determine whether the mechanism described above (Fig. 8) can account for the change in length distribution of sheared steady-state microtubules, we have applied this simulation to a scheme in which the probability is equal to 0.9859, for survival of the tubulin-GTP cap that is exposed when a disassembling microtubule loses all its tubulin-GDP subunits. The results from this simulation (Fig. 9) show that in 3300 s an initial length distribution, that is approximately bell-shaped length, is converted to an exponentially shaped distribution. The change in length distribution involves formation of a bimodal distribution of lengths (see 300-s curve), with peaks of very short and medium length microtubules. The latter population gets progressively longer, as the shape of the peak describing this population broadens. The agreement between the results from the stimulation (Fig. 9) and our experiments (Fig. 7) indicates that the mechanism described in Fig. 8 can account for the observed changes in microtubule length.

*Comparison with Earlier Results*—Our observation that disassembling microtubules tend to disassemble almost to completion, so that the tubulin-GTP cap at the opposite microtubule end is exposed, appears to be in agreement with results of Mitchison and Kirschner (1), who found an approximately linear time dependence for microtubule length increases after shearing. These results (1) could be fit to a Monte Carlo simulation (15), in which it was assumed that the half-time for microtubule recapping was 42–105 s, so that the mean excursion for a disassembling microtubule would be

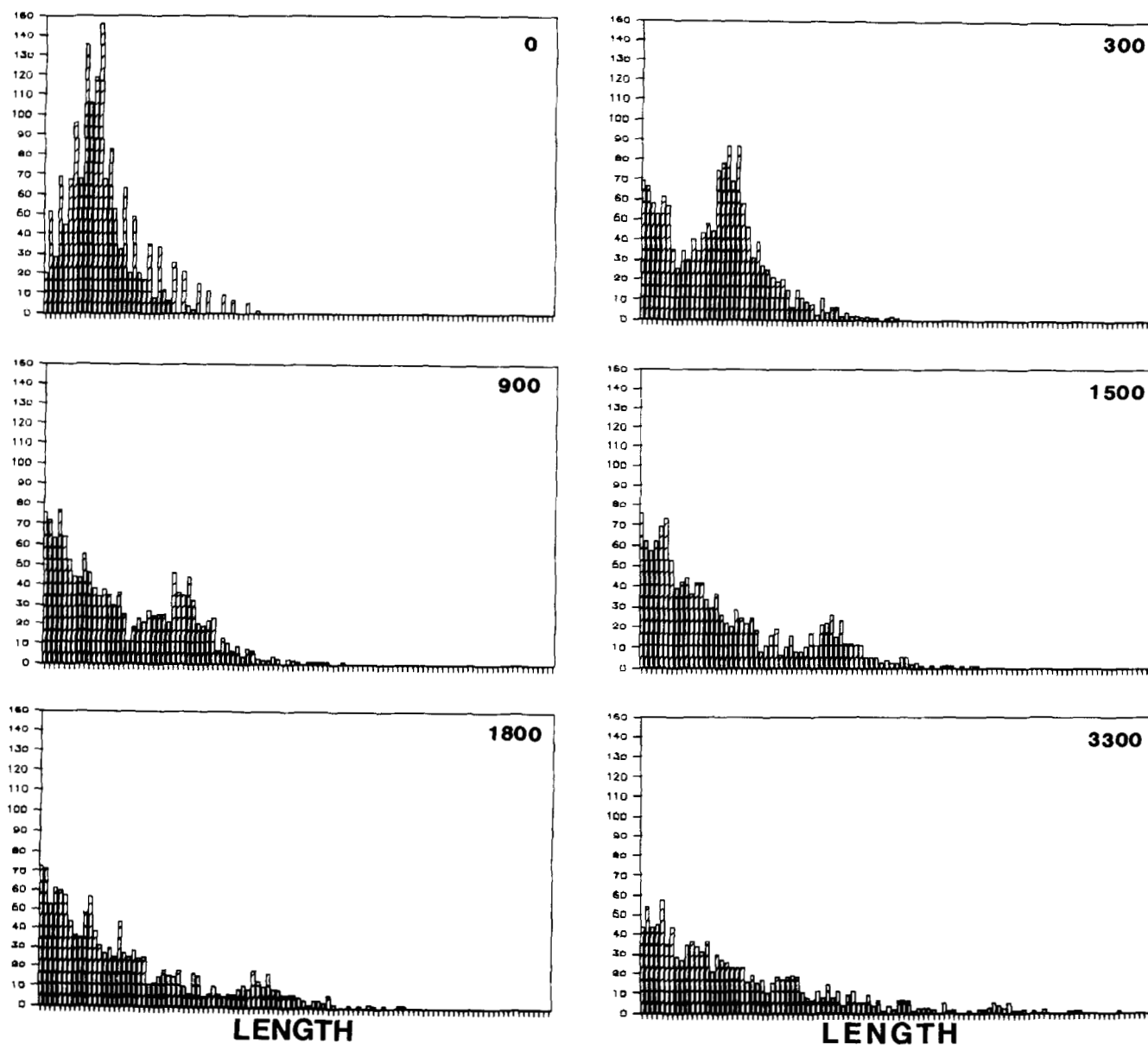


FIG. 9. Calculated length distribution of microtubules at varying times after shearing. The rate constants for tubulin-GTP gain and loss and for tubulin-GDP subunit loss at the two microtubule ends were as described previously (14). However, to make for longer excursions in length of uncapped microtubules, the rate constants for uncapping ( $k'$ ) and recapping ( $k$ ) were both made 10 times smaller. Most important, the probability of retention of the seed formed by exposure of the tubulin-GTP cap, generated by loss of all of the tubulin-GDP subunits from an uncapped microtubule was set equal to 0.9859. This probability is equal to  $1 - [\gamma/(\gamma + J_{11})]$ ;  $\gamma$  was set equal to 1 and  $J_{11}$  is 69.7. In the previous calculation (Fig. 5 in Ref. 14),  $\gamma$  was set equal to 10,000, so that seeds almost always disappear. Starting with 1,550 microtubules, the number of microtubules remaining was 1,491 at 300 s, 1,388 at 900 s, 1,319 at 1,500 s, 1,278 at 1,800 s, and 1,113 at 3,300 s. In the previous calculation (14) only 342 microtubules remain at 3,300 s. The range of the *abscissa* is from 0 to 172  $\mu\text{m}$ , for all figures.

12.6–31.4  $\mu\text{m}$  at the plus end and 7.8–13.6  $\mu\text{m}$  at the minus end (see above for the formula used to calculate this). Such large excursion would generate an approximately linear time dependence for an increase in length. We are unable to account for the relatively limited disassembly observed in another *in vitro* study (3), or the *in vivo* results (4), where relatively facile recapping occurs. The rate of recapping of disassembling microtubules may be extremely sensitive to reaction conditions, especially the presence of MAPs (2) and this may account for the *in vivo* results. Finally, in the Monte Carlo simulation (15) of microtubule length changes (1), the results could be accounted for by a scheme in which the probability for disappearance of the exposed tubulin-GTP cap

formed from disassembling microtubules was either near zero, or as high as 0.54. A probability of 0.87 did not fit the results, because it predicted a transient bimodal length distribution seen here (Fig. 7), but not in the earlier study (1). The difference between the results obtained here and previously (1) may be related to a difference in the size of the tubulin-GTP caps at microtubule ends. The number of tubulin-GTP subunits in the cap depends on the rate of addition and loss of tubulin-GTP subunits and the GTPase rate. A change in any of these parameters by a small difference in reaction conditions will modify the size of the tubulin-GTP cap. If the cap was smaller in the previous study (1), it would be less likely to survive to renucleate microtubules, as observed here.



*The Mechanism for Dynamic Instability*—The important point here is not that tubulin-GTP subunits in solution are reactive with a remnant tubulin-GTP cap, but that there is a remnant tubulin-GTP cap when microtubules disassemble. Although dynamic instability has been accounted for as resulting because microtubules are structurally inhomogeneous, with a number of tubulin-GTP subunits acting to cap each end (16), there is no compelling evidence for this structural inhomogeneity. Results from recent studies of the kinetics of microtubule assembly and GTPase reaction (17, 18) suggest that the tubulin-GTP cap may be a minimal structure, with perhaps only a single tubulin-GTP subunit at each end of the five helices that serve as elongation sites. The existence of such a minimal tubulin-GTP cap is ruled out by our observations, which require that the remnant tubulin-GTP cap generated from disassembly have the stability of a microtubule nucleating site; we do not expect that a stable nucleating site can be generated from five tubulin-GTP subunits, oriented as the five helices that serve as elongation sites.

*Acknowledgments*—We are grateful to Dr. Y. D. Chen for providing us with the computer program for the Monte Carlo simulation of microtubule dynamics.

## REFERENCES

1. Mitchison, T., and Kirschner, M. (1984) *Nature* **312**, 237-242
2. Horio, T., and Hotani, H. (1986) *Nature* **321**, 605-607
3. Farrell, K. W., Jordan, M. A., Miller, H. P., and Wilson, L. (1987) *J. Cell Biol.* **104**, 1035-1046
4. Sammak, P. J., Gorbsky, G. J., and Borisy, G. G. (1987) *J. Cell Biol.* **104**, 395-405
5. Caplow, M., Shanks, J., and Ruhlen, R. L. (1988) *J. Biol. Chem.* **263**, 10344-10352
6. Hill, T. L. (1985) *Proc. Natl. Acad. Sci. U. S. A.* **82**, 431-435
7. Zeeberg, B., Cheek, J., and Caplow, M. (1980) *Anal. Biochem.* **104**, 321-327
8. Williams, R. C., Jr., and Detrich, H. W., III (1979) *Biochemistry* **18**, 2499-2503
9. Karr, T. L., Kristofferson, D., and Purich, D. L. (1980) *J. Biol. Chem.* **255**, 8560-8566
10. Kristofferson, D., Karr, T. L., and Purich, D. L. (1980) *J. Biol. Chem.* **255**, 8567-8572
11. Caplow, M., Shanks, J., and Brylawski, B. P. (1986) *J. Biol. Chem.* **262**, 16233-16240
12. Johnson, K. A., and Borisy, G. G. (1977) *J. Mol. Biol.* **117**, 1-31
13. Kristofferson, D., Mitchison, T., and Kirschner, M. (1986) *J. Cell Biol.* **102**, 1007-1019
14. Chen, Y.-D., and Hill, T. (1985) *Proc. Natl. Acad. Sci. U. S. A.* **82**, 4127-4131
15. Chen, Y., and Hill, T. L. (1985) *Proc. Natl. Acad. Sci. U. S. A.* **82**, 1131-1135
16. Kirschner, M., and Mitchison, T. (1986) *Cell* **45**, 329-342
17. O'Brien, T. E., Voter, W. A., and Erickson, H. P. (1987) *Biochemistry* **26**, 4148-4156
18. Carlier, M.-F., Didry, D., and Pantaloni, D. (1987) *Biochemistry* **26**, 4428-4437